X-Ray Absorption Spectrum of the N_2^+ Molecular Ion

R. Lindblad,[1,2,3] L. Kjellsson,[4,5] R. C. Couto,[6,7] M. Timm,[2,8] C. Bülow,[2,9] V. Zamudio-Bayer,[2] M. Lundberg,[6] B. von Issendorff,[9] J. T. Lau,[2,9] S. L. Sorensen,[1] V. Carravetta,[10] H. Ågren,[11,4,7,*] and J.-E. Rubensson[4,†]

[1]Department of Physics, Lund University, Box 118, SE-22100 Lund, Sweden
[2]Abteilung für Hochempfindliche Röntgenspektroskopie, Helmholtz-Zentrum Berlin für Materialien und Energie, Albert-Einstein-Str. 15, 12489 Berlin, Germany
[3]Inorganic Chemistry, Department of Chemistry—Ångström Laboratory, Uppsala University, SE-75121 Uppsala, Sweden
[4]Department of Physics and Astronomy, Uppsala University, Box 516, SE-751 20 Uppsala, Sweden
[5]European XFEL GmbH, Holzkoppel 4, 22869 Schenefeld, Germany
[6]Theoretical Chemistry, Department of Chemistry—Ångström Laboratory, Uppsala University, SE-75121 Uppsala, Sweden
[7]Theoretical Chemistry and Biology, School of Chemistry, Biotechnology and Health, Royal Institute of Technology, SE-106 91 Stockholm, Sweden
[8]Institut für Optik und Atomare Physik, Technische Universität Berlin, Hardenbergstr. 36, 10623 Berlin, Germany
[9]Physikalisches Institut, Albert-Ludwigs-Universität Freiburg, Hermann-Herder-Str. 3, 79104 Freiburg, Germany
[10]IPCF-CNR, via Moruzzi 1, 56124 Pisa, Italy
[11]College of Chemistry and Chemical Engineering, Henan University, Kaifeng, Henan 475004, People's Republic of China

The x-ray absorption spectrum of N_2^+ in the K-edge region has been measured by irradiation of ions stored in a cryogenic radio frequency ion trap with synchrotron radiation. We interpret the experimental results with the help of restricted active space multiconfiguration theory. Spectroscopic constants of the $1\sigma_u^{-1}\,^2\Sigma_u^+$ state, and the two $1\sigma_u^{-1}3\sigma_g^{-1}1\pi_g\,^2\Pi_u$ states are determined from the measurements. The charge of the ground state together with spin coupling involving several open shells give rise to double excitations and configuration mixing, and a complete breakdown of the orbital picture for higher lying core-excited states.

DOI: 10.1103/PhysRevLett.124.203001

X-ray absorption spectroscopy (XAS) of small molecular ions can become a powerful technique for fundamental molecular physics, with potential ramifications in several fields.

First, it gives more detailed information about core ionized states normally observed by x-ray photoelectron spectroscopy (XPS). XPS is widely used for studies of the electronic structure of matter, including atoms, molecules and clusters [1]. The insights available from high-resolution studies of core ionized states provide a foundation for understanding electronic structure and for developing theoretical models [2,3]. Photoionization of a neutral molecule and XAS of the corresponding molecular ion in the ground state lead partly to the same final states. In XAS, however, the dipole selection rule simplifies the interpretation of the spectrum and allows for a more detailed analysis. Here we show that this enables an accurate derivation of spectroscopic constants for states that are difficult to analyse with XPS.

Second, compared to the closed-shell neutral molecule the additional charge on the ion leads to an open shell, a deep average Coulomb potential and a high ionization potential. As we show here, XAS of the molecular ion therefore allows for the observation of highly excited states, which description challenges current theoretical models.

Third, a frontier of chemical physics is the investigation of charge migration dynamics in molecules [4]. To gain new insights into such ultrafast phenomena, pump-probe experiments using x-ray free-electron laser (FEL) sources are promising [5]. Typically, a system is ionized by a pump pulse, thereby initiating dynamic electronic and nuclear rearrangement which is probed by a second pulse in an XAS process. Understanding the complex data from such experiments relies on the availability of XAS reference data.

XAS has earlier been applied to molecular ions using various schemes of ion beam and trap techniques [6–11], the challenge being primarily the low target density. Here we meet this challenge using the nano cluster trap end station at beam line UE52-PGM at BESSY II, which hosts a unique experimental setup for x-ray spectroscopy of

size-selected and trapped cold ions [12–15]. We present the first x-ray absorption spectrum of the N_2^+ ion. This is measured with a spectral quality that allows for analysis of the vibrational excitations and for resolving close lying states. Our experimental observations are compared to predictions from state-of-the-art first-principle calculations.

Ionic molecular nitrogen was produced by leaking in N_2 gas into the He plasma produced in a magnetron sputter source. The cationic species were directed to a quadrupole mass filter, where the N_2^+ molecular ion was selected. The selected ions were guided to the ion trap, where they were accumulated and exposed to x-rays, and the trap content was extracted in short bunches to a reflectron time-of-flight mass spectrometer [12]. The trap was cooled to 15 K and the ions were thermalized in a helium buffer gas. While rotational and translational relaxation occurs quickly in collisions with the buffer gas, vibrational relaxation in N_2^+ is significantly slower [16–21], and vibrational excitations may survive during the trapping time of a few tens of seconds. The XAS signal is dominated by excitations of N_2^+ ions in the vibrational ground state, but a small part of the signal is associated with vibrationally excited states, which can be excited by the Penning ionization process in the ion source [22,23].

After x-ray absorption the core excited state primarily relaxes via Auger decay followed by dissociation. The product ions N^+ and N_2^{2+} (both having a mass/charge ratio of 14 amu) were used to record the action spectrum of N_2^+. In this case, N^+/N_2^{2+} was the only observed ion signal, and we assume that it is proportional to the x-ray absorption cross section [24,25]. Neutral N_2 was measured in an upstream gas cell. The energy resolution of our

vibrationally resolved measurements was 50 meV and the absolute energies are given with an uncertainty of less than 20 meV. For further experimental details, see the Supplemental Material [26].

To simulate the K-shell excitation spectrum, electronic structure calculations, including transition energies and intensities were performed. In addition, calculations of the potential energy curves were performed for the states assigned to the features below 405 eV. Based on these potential energy curves wave packet calculations were done to predict the vibrational fine structure in the spectra. The wave packet calculations were performed with the RAM software [32–34] and the electronic structure was calculated with the OPENMOLCAS package [35]. All electronic excited states were computed with the restricted active space self-consistent field (RASSCF) [36–38] method, followed by a second-order pertubation (RASPT2) [39], using the multistate formalism considering the ANO-RCC-VTZP basis set along with the auxiliary (8s6p4d) Rydberg basis set. Calculations were performed in the Abelian point group C_{2v} and the orbitals were localized by the PIPEK-MEZEY procedure [40]. Core-excited states were obtained using the core-valence separation (CVS) method implemented in the OPENMOLCAS code [41] and the transition dipole moments were obtained by the RAS state-interaction approach [42,43]. Detailed information about active spaces, theoretical energy shifts, as well as energy, oscillator strengths and assignments of all calculated electronic states are found in the Supplemental Material [26].

The x-ray absorption spectrum of N_2^+ (Fig. 1) shows a sharp and structured feature at approximately 394 eV, a strong double feature peaking at 402 and 403 eV followed by a number of weak structures in the 405–424 eV region.
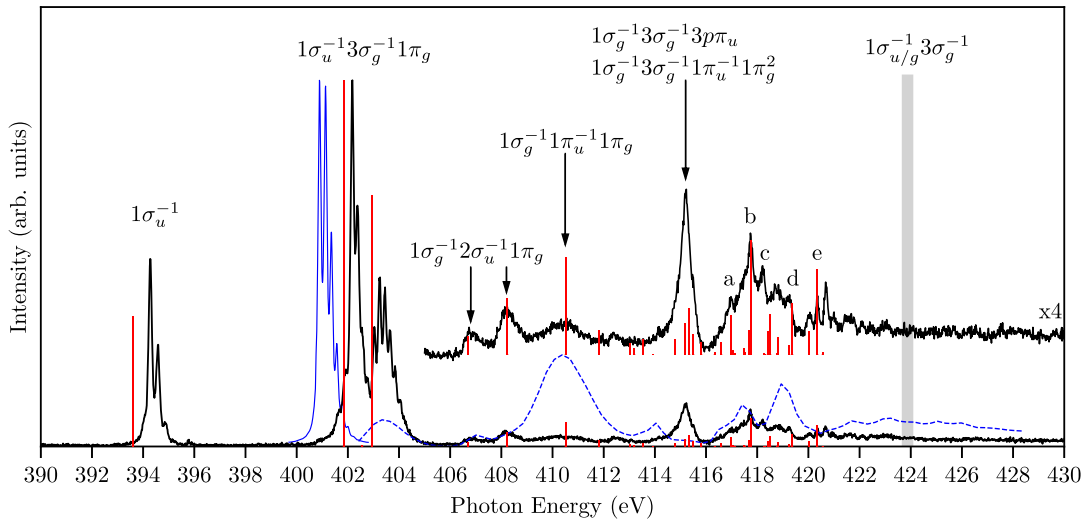
FIG. 1. The x-ray absorption spectrum of N_2^+ (solid black) and N_2 (solid blue) and the calculated spectrum of N_2^+ (solid red bars). The theoretical spectrum is shifted by -2.43 eV to match the region above 405 eV. For comparison we show the N_2 photoionization shake-up spectrum (dotted blue line), from Ref. [44], reversed in energy to fit the photon energy scale and shifted by the negative of the N_2 ionization energy.
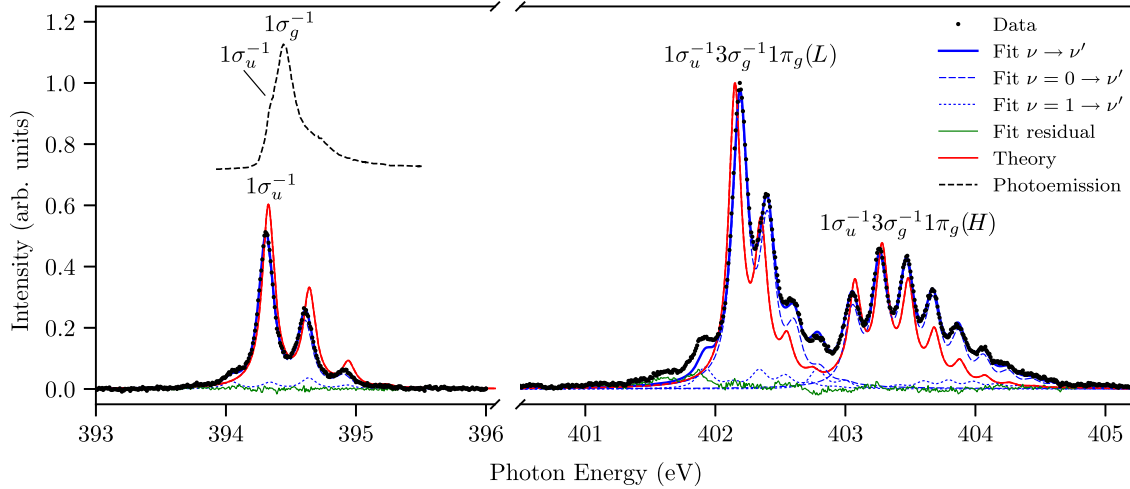
FIG. 2. The transitions to the $1\sigma_u^{-1}\,^2\Sigma_u^+$ state (left) and the two $1\sigma_u^{-1}3\sigma_g^{-1}1\pi_g\,^2\Pi_u$ states (right), where L and H denote lower, respectively higher, energy. The figure shows the experimental data (black dots), the curve fit for the Franck-Condon analysis (blue line) with the contribution from the ground state, $\nu = 0$, and the first vibrationally excited state $\nu = 1$ (dashed blue lines) and the theoretical spectra obtained from the calculated potential energy curves (red line). We also show the corresponding photoelectron spectrum of N_2 (dashed black line), from Ref. [47], plotted on the photon energy scale and shifted by the negative of the ionization energy. The theoretical spectra are shifted by -0.47 eV.

We assign the fine structure of the first three features to vibronic excitations.

The ground state of the neutral molecule is $1\sigma_g^2 1\sigma_u^2 2\sigma_g^2 2\sigma_u^2 1\pi_u^4 3\sigma_g^2\,^1\Sigma_g^+$, and its ionization energy is 15.58 eV [45,46]. In the cation the uppermost $3\sigma_g$ orbital is only singly occupied and we expect the first core excited state to be due to a $1\sigma_u \to 3\sigma_g$ transition. This leaves the system in a $^2\Sigma_u^+$ state, with a closed valence shell and a vacancy in the *ungerade* core orbital. The same final state is reached in inner-shell photoionization of neutral N_2 [47] or x-ray-emission-threshold-electron coincidence spectroscopy of neutral N_2, which determines the $\nu = 0 \to \nu' = 0$ excitation energy to be 409.82 eV [48]. Therefore, we expect the corresponding XAS resonance in the molecular ion at $409.82 - 15.58$ eV $= 394.24$ eV, in close agreement with the observed $\nu = 0 \to \nu' = 0$ transition at an energy of 394.29 ± 0.02 eV. A Franck-Condon analysis assuming Morse potentials was performed, see Fig. 2, and the resulting spectroscopic constants are found in Table I. In order to reproduce the transitions in the spectrum, the Franck-Condon analysis was carried out with both $\nu = 0$ and $\nu = 1$ in the initial state, with the latter corresponding to approximately 11% of the total intensity. For the $1\sigma_u^{-1}\,^2\Sigma_u^+$ state, Ehara *et al.* [49] report a harmonic frequency of 297.93 ± 3.5 meV, similar to our experimental value of 302.6 ± 3.8 meV. No experimental value of the anharmonicity is however given. Our experimental life time broadening of 113 ± 4 meV is similar to the value 113 ± 2 meV obtained for the N_2 $(N1s, \nu = 0) \to (\pi_g^*, \nu')$ transition [50]. Only an approximate life time broadening of 102 ± 10 meV has earlier been reported for a transition to the $1\sigma_u^{-1}\,^2\Sigma_u^+$ final state [47].

In contrast to XPS where both ungerade and gerade states contribute, only the ungerade final states are dipole allowed, which facilitates determination of the spectroscopic constants. This becomes clear when comparing the transition to the $1\sigma_u^{-1}\,^2\Sigma_u^+$ final state with the corresponding XPS spectrum [47] in Fig. 2. In the XPS spectrum, the vibrations are clearly more challenging to resolve due to the gerade-ungerade energy split of about 100 meV [47]. Compared to XAS, XPS has an increased experimental broadening resulting from the spectrometer energy resolution. In addition, XAS does not suffer from complications due to postcollision effects, which are strong at close-to-threshold ionization, or due to limitations in experimental throughput and resolving power, which are notorious far above threshold. Due to these reasons the present method for characterization of core-ionized states has advantages compared to XPS.

The features with the $\nu = 0 \to \nu' = 0$ transition at energies of 402.21 ± 0.02 eV and 403.08 ± 0.02 eV correspond to the π^* excitation well known from the XAS spectrum of neutral nitrogen, but with a $3\sigma_g$ spectator hole in the case of the ion, i.e., a $3\sigma_g^{-1}\,^2\Sigma_g \to 1\sigma_u^{-1}3\sigma_g^{-1}1\pi_g\,^2\Pi_u$ transition. We see a splitting of the $1\sigma_u^{-1}3\sigma_g^{-1}1\pi_g\,^2\Pi_u$ state, due to two possible spin couplings. This has previously only been observed for N_2 as shake-up states in XPS [44,49,52,53], but overlapping $^2\Pi_u$ and $^2\Pi_g$ states have prohibited a detailed analysis, such as determining the spectroscopic constants. Here these states are resonantly excited, and the validity of the dipole approximation ensures that the $^2\Pi_u$ states are selected in the resonances. This enables a Franck-Condon analysis and the result is shown in Table I and in Fig. 2. Our theoretical

TABLE I. Experimental spectroscopic constants of core-hole excited N_2^+ as obtained by a Franck-Condon analysis assuming Morse potentials for the initial and final state, with the initial state defined by the vibrational constants from Laher and Gilmore [51]. T_e denotes the bottom of the potential curve, ω_e the harmonic frequency, $\omega_e\chi_e$ the anharmonicity coefficient, R_e the bond length and γ the life time broadening. The uncertainty is estimated from the largest variation achieved when vibrational excitations in the initial state are disregarded. For T_e the fitting error is much smaller than the experimental energy uncertainty of 20 meV. Theoretical vibrational constants are associated with the calculated potential energy curves presented in the Supplemental Material [26] and the theoretical T_e values are shifted by -0.47 eV.

	Experiment					Theory				
State	T_e [eV]	ω_e [meV]	$\omega_e\chi_e$ [meV]	ΔR_e [Å]	γ [meV FWHM]	T_e [eV]	ω_e [meV]	$\omega_e\chi_e$ [meV]	R_e [Å]	ΔR_e [Å]
$3\sigma_g^{-1}\,^2\Sigma_g^+$	0	$\cdots$	$\cdots$	$\cdots$	$\cdots$	0	268.78	2.12	1.12	$\cdots$
$1\sigma_u^{-1}\,^2\Sigma_u^+$	394.28	302.6 ± 3.8	1.35 ± 0.24	-0.040 ± 0.002	113 ± 4	394.30	311.64	2.94	1.08	-0.04
$1\sigma_u^{-1}3\sigma_g^{-1}1\pi_g\,^2\Pi_u$ (L)	402.24	218.8 ± 4.2	3.27 ± 2.7	0.051 ± 0.001	119 ± 9	402.19	212.15	3.39	1.17	0.05
$1\sigma_u^{-1}3\sigma_g^{-1}1\pi_g\,^2\Pi_u$ (H)	403.11	215.4 ± 2.5	2.27 ± 0.49	0.095 ± 0.001	115 ± 5	403.10	214.53	2.45	1.21	0.09

spectroscopic constants show excellent agreement with the experimental values, better than earlier theoretical predictions [49].

An example of a neutral diatomic molecule where spin-split two-hole-one-particle core-hole states are observed is the σ^* resonance in O_2, which is complicated due to ultrafast dissociation and Rydberg-valence mixing, and it has been intensely debated over the years [54]. In XAS of small open-shell molecular ions we expect that excitation to such states are common, and as shown here for N_2^+ they can be studied in more detail compared to XPS, by virtue of dipole selectivity.

The splitting between the two $1\sigma_u^{-1}3\sigma_g^{-1}1\pi_g\,^2\Pi_u$ states is determined by the exchange interaction between each pair of open shell orbitals. The analysis of the combination of determinants giving the two doublet states is in agreement with Hund's rule for the valence coupling, and thus suggests that the valence exchange interaction is stronger than the core-valence interaction. The experimentally observed exchange splitting between the vibrational ground states is 0.87 eV, close to our theoretical result of 0.91 eV. In the independent particle approximation, the intensity ratio between the two states is predicted as $I_L/I_H = 2.1$ where $L(H)$ denotes the lower (higher) energy state (see the Supplemental Material for further details [26,55]). The extended RASSCF calculation, including dynamic electron correlation, predicts however a ratio of 1.2, quite close to the experimental value 1.1.

At higher photon energies, above 405 eV, one might expect a phenomenon seen in XAS of neutral molecules [56], i.e., a dominance of one-electron transitions to Rydberg series converging to the ionization limits, and possibly to $3\sigma_u$, the next unoccupied molecular orbital. In contrast, we encounter double excitations and transitions to correlated states. For neutral N_2, double excitations are found above the ionization threshold [57–60], but in the ion they are found far below this threshold. The difference is largely due to the open shell nature of the ion as well as an increased Coulomb potential due to the additional hole in the cation, which shifts the ionization threshold higher. This is a general trend when comparing XAS of neutrals and positively charged molecular ions, similar to what is seen in the atomic case [61,62]. For N_2^+ the picture is exceedingly complicated due to the coupling between states and mixing of two-hole-one-particle Rydberg configurations, as well as three-hole-two-particle configurations, as will be discussed below. For all observed higher energy peaks we find however possible assignments.

In the 406–416 eV region we observe several broad peaks which are assigned to double excitations by our theory. A "π^*" excitation is here combined with the initial $3\sigma_g$ vacancy being filled by an electron from the $2\sigma_u$ (407 and 408.5 eV) or $1\pi_u$ (410 eV) orbital. As for the $1\sigma_u^{-1}3\sigma_g^{-1}1\pi_g\,^2\Pi_u$ final state, the double structure of the $3\sigma_g^{-1}\,^2\Sigma_g^+ \rightarrow 1\sigma_g^{-1}2\sigma_u^{-1}1\pi_g\,^2\Pi_u$ resonances indicates two possible spin couplings. We observe a significant broadening without fine structure suggesting that substantial nuclear dynamics is initiated in the excited states. In particular the transition to the $1\sigma_g^{-1}1\pi_u^{-1}1\pi_g\,^2\Sigma_u^{+/-}$ state is broad and structure-less. This transition corresponds to the most intense peak in the photoionization shake-up spectrum, which also is assigned to core hole final states with an additional $1\pi_u \rightarrow 1\pi_g$ excitation [44]. Our theory assigns the intense feature just above 415 eV to a collection of transitions into Rydberg $1\sigma_g^{-1}3\sigma_g^{-1}3p\pi_u\,^2\Pi_u$ and $1\sigma_u^{-1}3\sigma_g^{-1}1\pi_u^{-1}1\pi_g^2\,^2\Sigma_u^+$ states where the former dominates.

The 416–423 eV region shows a complex structure with a multitude of peaks. The theoretical analysis shows that this is due to transitions to highly correlated states, which have no leading configuration. In Fig. 1 the most intense states are labeled (a)–(e), and the contributions from different configurations are shown in Table II. Tentative assignments of all transitions are found in Supplemental Material [26]. It is important to notice that the complicated spectral structure above 416 eV contains a large number of

TABLE II. Approximate assignments for peaks (a)–(e) in Figure 1, based on configuration interaction (CI).

Peak	CI weight (%)	Assignment
(a)	48	$1\sigma_g^{-1}3\sigma_g^{-1}4s\sigma_u$
	20	$1\sigma_g^{-1}1\pi_u^{-1}3p\pi_u$
(b)	69	$1\sigma_u^{-1}3\sigma_g^{-1}4p\pi_g$
	37	$1\sigma_g^{-1}3\sigma_g^{-1}4s\sigma_u$
	19	$1\sigma_g^{-1}1\pi_u^{-2}1\pi_g^2$
(c)	65	$1\sigma_u^{-1}3\sigma_g^{-1}4p\pi_g$
	44	$1\sigma_g^{-2}2\sigma_u^{-1}3\sigma_g^{-1}1\pi_g^2$
	14	$1\sigma_g^{-1}1\pi_u^{-2}1\pi_g^2$
(d)	50	$1\sigma_g^{-1}2\sigma_u^{-1}1\pi_u^{-1}1\pi_g^2$
	22	$1\sigma_g^{-1}3\sigma_g^{-1}1\pi_u^{-1}1\pi_g^2$
(e)	38	$1\sigma_u^{-1}3\sigma_g^{-1}1\pi_u^{-1}1\pi_g^2$
	23	$1\sigma_u^{-1}2\sigma_u^{-1}1\pi_u^{-1}1\pi_g^2$

transitions as well as the presence of multiple curve crossings and avoided crossings. The accuracy of our calculated intensities will therefore be limited by the neglect of spin-orbit and nonadiabatic couplings. For many of these transitions Rydberg and doubly occupied $1\pi_g$ final state configurations are involved. We note however that the assignments in this energy region is dependent on the active space used in the calculations. With 19 orbitals in the active space instead of the 24 used here, many states in this energy region are associated with a $1\sigma_g \rightarrow 3\sigma_u$ transition. This again highlights the challenge for theory to correctly describe this part of the spectrum. We also note that the spectrum does not contain Rydberg series converging all the way to the ionization thresholds, which is common in XAS spectra of small neutral molecules [56]. The calculated ionization thresholds for the four singlet-triplet and gerade-ungerade split combinations are in the 423.6–424.1 eV range, marked in Fig. 1 as a vertical broad gray line.

The single electron excitation picture has, even though it is a simplification, been instrumental in interpreting molecular XAS. It is also the foundation of useful interpreting models and structure-property relationships, like the effective one-center rule and the building block principle [63]. In contrast, many-body effects, although early identified in XAS or EELS for a few small molecules [64,65], appear only as faint and often hardly visible spectral structures. For N_2^+ XAS, the situation is drastically different—here we have identified only one transition as a pure single electron excitation, six transitions with a leading one-electron configuration but still significantly correlated, and a large number of final states that have multielectron character associated with a complete breakdown of the molecular orbital picture.

In summary, the x-ray absorption spectrum of the molecular ion N_2^+ has been measured and analyzed.

This allows for a detailed characterization of the first three core excited states, and identification of double excitations and extensive configuration mixing closer to the ionization limit. The phenomenology of XAS of molecular ions is qualitatively different from XAS of neutral molecules. The difference is largely due to the open-shell nature of the ion and the deeper Coulomb potential in the final states. For N_2^+ this leads to a multitude of bound core hole states, and a complete breakdown of the orbital picture. We expect that the complications are quite general, and that XAS of molecular ions with the experimental data quality demonstrated here, is a new arena for investigation of highly excited molecular states.

---

[*]hagren@kth.se
[†]jan-erik.rubensson@physics.uu.se

[1] K. Siegbahn *et al.*, *ESCA Applied to Free Molecules* (North-Holland Pub. Co., Amsterdam, 1969).

[2] M. Patanen, S. Svensson, and N. Mårtensson, Electron spectroscopy using ultra brilliant synchrotron X-ray sources, J. Electron Spectrosc. Relat. Phenom. **200**, 78 (2015), Special Anniversary Issue.

[3] R. Püttner and K. Ueda, The angularly resolved O 1s ion-yield spectrum of O_2 revisited, J. Chem. Phys. **145**, 224302 (2016).

[4] H. J. Wörner, C. A. Arrell, N. Banerji, A. Cannizzo, M. Chergui, A. K. Das, P. Hamm, U. Keller, P. M. Kraus, E. Liberatore, P. Lopez-Tarifa, M. Lucchini, M. Meuwly, C. Milne, J.-E. Moser, U. Rothlisberger, G. Smolentsev, J. Teuscher, J. A. van Bokhoven, and O. Wenger, Charge migration and charge transfer in molecular systems, Struct. Dyn. **4**, 061508 (2017).

[5] L. Young *et al.*, Roadmap of ultrafast x-ray atomic and molecular physics, J. Phys. B **51**, 032003 (2018).

[6] J.-P. Mosnier, E. T. Kennedy, P. van Kampen, D. Cubaynes, S. Guilbaud, N. Sisourat, A. Puglisi, S. Carniato, and J.-M. Bizau, Inner-shell photoexcitations as probes of the

molecular ions CH^+, OH^+, and SiH^+: Measurements and theory, Phys. Rev. A **93**, 061401(R) (2016).

[7] T. Andersen, H. Kjeldsen, H. Knudsen, and F. Folkmann, Absolute cross section for photoionization of CO^+ leading to longlived metastable CO^{2+}, J. Phys. B **34**, L327 (2001).

[8] G. Hinojosa, A. M. Covington, R. A. Phaneuf, M. M. Sant'Anna, R. Hernandez, I. R. Covington, I. Domínguez, J. D. Bozek, A. S. Schlachter, I. Álvarez, and C. Cisneros, Formation of long-lived CO^{2+} via photoionization of CO^+, Phys. Rev. A **66**, 032718 (2002).

[9] S. Klumpp, A. A. Guda, K. Schubert, K. Mertens, J. Hellhund, A. Müller, S. Schippers, S. Bari, and M. Martins, Photoabsorption of the molecular IH cation at the iodine $3d$ absorption edge, Phys. Rev. A **97**, 033401 (2018).

[10] S. Bari, L. Inhester, K. Schubert, K. Mertens, J. O. Schunck, S. Dörner, S. Deinert, L. Schwob, S. Schippers, A. Müller, S. Klumpp, and M. Martins, Inner-shell X-ray absorption spectra of the cationic series $NH_y^+ (y = 0 - 3)$, Phys. Chem. Chem. Phys. **21**, 16505 (2019).

[11] E. T. Kennedy, J. P. Mosnier, P. Van Kampen, J. M. Bizau, D. Cubaynes, S. Guilbaud, S. Carniato, A. Puglisi, and N. Sisourat, Vibrational effects in the photo-ion yield spectrum of the SiH_2^+ molecular ion following 2p inner-shell excitation, J. Phys. Conf. Ser. **1289**, 012003 (2019).

[12] K. Hirsch, J. T. Lau, Ph. Klar, A. Langenberg, J. Probst, J. Rittmann, M. Vogel, V. Zamudio-Bayer, T. Möller, and B. von Issendorff, X-ray spectroscopy on size-selected clusters in an ion trap: From the molecular limit to bulk properties, J. Phys. B **42**, 154029 (2009).

[13] M. Niemeyer, K. Hirsch, V. Zamudio-Bayer, A. Langenberg, M. Vogel, M. Kossick, C. Ebrecht, K. Egashira, A. Terasaki, T. Möller, B. v. Issendorff, and J. T. Lau, Spin Coupling and Orbital Angular Momentum Quenching in Free Iron Clusters, Phys. Rev. Lett. **108**, 057201 (2012).

[14] A. Langenberg, K. Hirsch, A. Ławicki, V. Zamudio-Bayer, M. Niemeyer, P. Chmiela, B. Langbehn, A. Terasaki, B. v. Issendorff, and J. T. Lau, Spin and orbital magnetic moments of size-selected iron, cobalt, and nickel clusters, Phys. Rev. B **90**, 184420 (2014).

[15] V. Zamudio-Bayer, R. Lindblad, C. Bülow, G. Leistner, A. Terasaki, B. v. Issendorff, and J. T. Lau, Electronic ground state of Ni_2^+, J. Chem. Phys. **145**, 194302 (2016).

[16] S. Kato, V. M. Bierbaum, and S. R. Leone, Laser fluorescence and mass spectrometric measurements of vibrational relaxation of $N_2^+(\nu)$ with He, Ne, Ar, Kr, and Xe, Int. J. Mass Spectrom. Ion Process. **149–150**, 469 (1995), honour Biography David Smith.

[17] S. Chakrabarty, M. Holz, E. K. Campbell, A. Banerjee, D. Gerlich, and J. P. Maier, A novel method to measure electronic spectra of cold molecular ions, J. Phys. Chem. Lett. **4**, 4051 (2013).

[18] S. De Benedictis, G. Dilecce, and M. Simek, Vibrational excitation of $N_2^+(B, \nu)$ in $He - N_2$ pulsed RF discharges, J. Phys. B **27**, 615 (1994).

[19] L. G. Piper and W. J. Marinelli, Determination of non Boltzmann vibrational distributions of $N_2(X, \nu')$ in He/N_2 microwave-discharge afterglows, J. Chem. Phys. **89**, 2918 (1988).

[20] J. Jolly, M. Touzeau, and A. Ricard, Determination of non-Boltzmann vibrational level populations of excited nitrogen

using the Penning ionisation technique, J. Phys. B **14**, 473 (1981).

[21] W. C. Richardson and D. W. Setser, Penning ionization optical spectroscopy: Metastable helium (He $2\,^3S$) atoms with nitrogen, carbon monoxide, oxygen, hydrogen chloride, hydrogen bromide, and chlorine, J. Chem. Phys. **58**, 1809 (1973).

[22] H. Sekiya, T. Hirayama, M. Endoh, M. Tsuji, and Y. Nishimura, Laser-induced fluorescence detection of $N^+_2(X^2\Sigma^+_g)$ resulting from the $He(2^3S) + N_2$ and He^+, $He^+_2 + N_2$ reactions in a flowing afterglow, Chem. Phys. **101**, 291 (1986).

[23] D. C. Dunlavy and P. E. Siska, Probing the transition state of the $He^*(2^1S) + N_2$ penning ionization reaction with electron spectroscopy, J. Phys. Chem. **100**, 21 (1996).

[24] W. Eberhardt, J. Stöhr, J. Feldhaus, E. W. Plummer, and F. Sette, Correlation between Electron Emission and Fragmentation into Ions Following Soft-X-Ray Excitation of the N_2 Molecule, Phys. Rev. Lett. **51**, 2370 (1983).

[25] I. H. Suzuki and N. Saito, Fragmentation of N_2 in the inner-shell to Rydberg-orbital excited states $(K)^{-1}(nl)^1$, J. Chem. Phys. **91**, 5324 (1989).

[26] See the Supplemental Material at http://link.aps.org/supplemental/10.1103/PhysRevLett.124.203001 for experimental and theoretical details, potential energy curves, and comments on the intensity ratio of the $1\sigma_u^{-1}3\sigma_g^{-1}1\pi_g\,^2\Pi_u$ states, which includes Refs. [27–31].

[27] M. R. Weiss, R. Follath, K. J. S. Sawhney, and T. Zeschke, Absolute energy calibration for plane grating monochromators, Nucl. Instrum. Methods Phys. Res., Sect. A **467–468**, 482 (2001).

[28] K. C. Prince, M. Vondráček, J. Karvonen, M. Coreno, R. Camilloni, L. Avaldi, and M. De Simone, A critical comparison of selected 1s and 2p core hole widths, J. Electron Spectrosc. Relat. Phenom. **101–103**, 141 (1999).

[29] R. N. S. Sodhi and C. E. Brion, Reference energies for inner shell electron energy-loss spectroscopy, J. Electron Spectrosc. Relat. Phenom. **34**, 363 (1984).

[30] P. M. Morse, Diatomic molecules according to the wave mechanics. II. Vibrational levels, Phys. Rev. **34**, 57 (1929).

[31] J. P. Dahl and M. Springborg, The Morse oscillator in position space, momentum space, and phase space, J. Chem. Phys. **88**, 4535 (1988).

[32] P. Sałek, F. Gel'mukhanov, and H. Ågren, Wave-packet dynamics of resonant x-ray Raman scattering: Excitation near the Cl $L_{\text{II,III}}$ edge of HCl, Phys. Rev. A **59**, 1147 (1999).

[33] F. Gel'mukhanov and H. Ågren, Resonant X-ray Raman scattering, Phys. Rep. **312**, 87 (1999).

[34] R. C. Couto, M. Guarise, A. Nicolaou, N. Jaouen, G. S. Chiuzbăian, J. Lüning, V. Ekholm, J.-E. Rubensson, C. Såthe, F. Hennies et al., Coupled electron-nuclear dynamics in resonant $1\sigma \rightarrow 2\pi$ x-ray Raman scattering of CO molecules, Phys. Rev. A **93**, 032510 (2016).

[35] I. F. Galván, M. Vacher, A. Alavi, C. Angeli, F. Aquilante, J. Autschbach, J. J. Bao, S. I. Bokarev, N. A. Bogdanov, and R. K. Carlson et al., Openmolcas: From source code to insight, J. Chem. Theory Comput. **15**, 5925 (2019).

[36] H. Jørgen Aa Jensen, P. Jørgensen, and H. Ågren, Efficient optimization of large scale MCSCF wave functions with a restricted step algorithm, J. Chem. Phys. **87**, 451 (1987).

[37] P. Åke Malmqvist, A. Rendell, and B. O. Roos, The restricted active space self-consistent-field method, implemented with a split graph unitary group approach, J. Phys. Chem. **94**, 5477 (1990).

[38] H. Ågren, A. Flores-Riveros, and H. J. A. Jensen, An efficient method for calculating molecular radiative intensities in the VUV and Soft X-ray wavelength regions, Phys. Scr. **40**, 745 (1989).

[39] P. Åke Malmqvist, K. Pierloot, A. R. M. Shahi, C. J. Cramer, and L. Gagliardi, The restricted active space followed by second-order perturbation theory method: Theory and application to the study of CuO_2 and Cu_2O_2 systems, J. Chem. Phys. **128**, 204109 (2008).

[40] J. Pipek and P. G. Mezey, A fast intrinsic localization procedure applicable for abinitio and semiempirical linear combination of atomic orbital wave functions, J. Chem. Phys. **90**, 4916 (1989).

[41] M. G. Delcey, L. K. Sørensen, M. Vacher, R. C. Couto, and M. Lundberg, Efficient calculations of a large number of highly excited states for multiconfigurational wavefunctions, J. Comput. Chem. **40**, 1789 (2019).

[42] P.-Å. Malmqvist and B. O. Roos, The CASSCF state interaction method, Chem. Phys. Lett. **155**, 189 (1989).

[43] P. Å. Malmqvist, B. O. Roos, and B. Schimmelpfennig, The restricted active space (RAS) state interaction approach with spin–orbit coupling, Chem. Phys. Lett. **357**, 230 (2002).

[44] S. Svensson, A. Naves de Brito, M. P. Keane, N. Correia, L. Karlsson, C. M. Liegener, and H. Ågren, The N 1s core electron shake-up and the shake-up Auger satellite spectrum of the N_2 molecule, J. Phys. B **25**, 135 (1992).

[45] P. Baltzer, M. Larsson, L. Karlsson, B. Wannberg, and M. C. Göthe, Inner-valence states of N_2^+ studied by uv photoelectron spectroscopy and configuration-interaction calculations, Phys. Rev. A **46**, 5545 (1992).

[46] T. Trickl, E. F. Cromwell, Y. T. Lee, and A. H. Kung, State-selective ionization of nitrogen in the $X^2\Sigma^+_g \nu_+ = 0$ and $\nu_+ = 1$ states by two-color $(1 + 1)$ photon excitation near threshold, J. Chem. Phys. **91**, 6006 (1989).

[47] U. Hergenhahn, O. Kugeler, A. Rüdel, E. E. Rennie, and A. M. Bradshaw, Symmetry-selective observation of the N 1s shape resonance in N_2, J. Phys. Chem. A **105**, 5704 (2001).

[48] M. Alagia, R. Richter, S. Stranges, M. Agåker, M. Ström, J. Söderström, C. Såthe, R. Feifel, S. Sörensen, A. De Fanis, K. Ueda, R. Fink, and J.-E. Rubensson, Core level ionization dynamics in small molecules studied by x-ray-emission threshold-electron coincidence spectroscopy, Phys. Rev. A **71**, 012506 (2005).

[49] M. Ehara, H. Nakatsuji, M. Matsumoto, T. Hatamoto, X. J. Liu, T. Lischke, G. Prümper, T. Tanaka, C. Makochekanwa, M. Hoshino, H. Tanaka, J. Harries, Y. Tamenori, and K. Ueda, Symmetry-dependent vibrational excitation in N 1 s photoionization of N_2: Experiment and theory, J. Chem. Phys. **124**, 124311 (2006).

[50] M. Kato, Y. Morishita, M. Oura, H. Yamaoka, Y. Tamenori, K. Okada, T. Matsudo, T. Gejo, I. H. Suzuki, and N. Saito, Absolute photoionization cross sections with ultra-high energy resolution for Ar, Kr, Xe and N2 in inner-shell ionization regions, J. Electron Spectrosc. Relat. Phenom. **160**, 39 (2007).

[51] R. R. Laher and F. R. Gilmore, Improved fits for the vibrational and rotational constants of many states of nitrogen and oxygen, J. Phys. Chem. Ref. Data **20**, 685 (1991).

[52] G. Angonoa, O. Walter, and J. Schirmer, Theoretical K shell ionization spectra of N_2 and CO by a fourth order Green's function method, J. Chem. Phys. **87**, 6789 (1987).

[53] M. Neeb, A. Kivimäki, B. Kempgens, H. M. Köppe, A. M. Bradshaw, and J. Feldhaus, Conjugate shake-up-enhanced Auger transitions in N_2, Phys. Rev. A **52**, 1224 (1995).

[54] R. Feifel, Y. Velkov, V. Carravetta, C. Angeli, R. Cimiraglia, P. Salek, F. Gelmukhanov, S. L. Sørensen, M. N. Piancastelli, A. De Fanis, K. Okada, M. Kitajima, T. Tanaka, H. Tanaka, and K. Ueda, X-ray absorption and resonant Auger spectroscopy of O_2 in the vicinity of the O 1s $\rightarrow \sigma*$ resonance: Experiment and theory, J. Chem. Phys. **128**, 064304 (2008).

[55] H. Ågren and V. Carravetta, The core electron shake phenomenon, Int. J. Quantum Chem. **42**, 685 (1992).

[56] J. i. Adachi, N. Kosugi, and A. Yagishita, Symmetry-resolved soft x-ray absorption spectroscopy: Its application to simple molecules, J. Phys. B **38**, R127 (2005).

[57] M. Neeb, A. Kivimäki, B. Kempgens, H. M. Köppe, K. Maier, A. M. Bradshaw, and N. Kosugi, Partial electron yield spectrum of N_2: Doubly excited states at the K-shell threshold, Chem. Phys. Lett. **320**, 217 (2000).

[58] Y. Hikosaka, T. Gejo, T. Tamura, K. Honma, Y. Tamenori, and E. Shigemasa, Core-valence multiply excited states in N_2 probed by detecting metastable fragments, J. Phys. B **40**, 2091 (2007).

[59] E. Shigemasa, T. Gejo, M. Nagasono, T. Hatsui, and N. Kosugi, Double and triple excitations near the K-shell ionization threshold of N_2 revealed by symmetry-resolved spectroscopy, Phys. Rev. A **66**, 022508 (2002).

[60] B. Kempgens, A. Kivimäki, M. Neeb, H. M. Käppe, A. M. Bradshaw, and J. Feldhaus, A high-resolution N 1s photoionization study of the molecule in the near-threshold region, J. Phys. B **29**, 5389 (1996).

[61] K. Hirsch, V. Zamudio-Bayer, F. Ameseder, A. Langenberg, J. Rittmann, M. Vogel, T. Möller, B. v. Issendorff, and J. T. Lau, $2p$ x-ray absorption of free transition-metal cations across the $3d$ transition elements: Calcium through copper, Phys. Rev. A **85**, 062501 (2012).

[62] S. Schippers, M. Martins, R. Beerwerth, S. Bari, K. Holste, K. Schubert, J. Viefhaus, D. Wolf Savin, S. Fritzsche, and A. Müller, Near L-edge single and multiple photoionization of singly charged iron ions, Astrophys. J. **849**, 5 (2017).

[63] J. Stöhr, *NEXAFS Spectroscopy* (Springer Verlag, Berlin, 1992).

[64] H. Ågren and R. Arneberg, Origin of fine structure in the vicinity of the K-edges in the CO electron energy loss spectra, Phys. Scr. **30**, 55 (1984).

[65] R. Arneberg, H. Ågren, J. Müller, and R. Manne, Multi-electron transitions in the K-shell electron energy loss spectrum of N_2, Chem. Phys. Lett. **91**, 362 (1982).